RSC Advances

ROYAL SOCIETY OF CHEMISTRY

www.rsc.org/advances

Journal Name

ARTICLE

Formation of surface cobalt structures in SiC-supported Fischer-Tropsch catalysts

Received 00th January 20xx,

Accepted 00th January 20xx

DOI: 10.1039/x0xx00000x

www.rsc.org/

I.G. Solomonik[a.1], K.O. Gryaznov[a], V.F. Skok[a], V.Z. Mordkovich[a, b]

The formation of surface cobalt structures was investigated for a number of β-SiC-supported Fischer-Tropsch catalysts. Several different supports were used, both pristine and alumina-modified β-SiC. The techniques of temperature-programmed reduction, nitrogen physisorption, thermal gravimetric analysis, heat conductivity and catalytic testing in Fischer-Tropsch synthesis were employed. It was determined that despite highly similar manufacturer specifications, differences in support genesis may lead to different porosities, surface cobalt phase compositions and catalytic activity, even with the use of identical catalyst preparation procedures. The control of the formation of the surface cobalt structure can also be realized by parameters of the catalyst preparation, such as one- or multi-step impregnation from aqueous or ethanol solution and annealing in air or helium flow or without gas flow. These findings open avenues of research for the optimization of the whole catalyst formation route on the basis of identification of the most efficient surface cobalt phase composition and realization of higher thermal conductivity.

[a] *Technological Institute for Superhard and Novel Carbon Materials, Troitsk, Moscow, Russia Address here.*
[b] *INFRA Technology LLC, Houston, USA.*
[1] Corresponding author. Tel.: +7499 400 62 25 int. 372; fax: +7499 400 62 60
E-mail addresses: solomonik@tisnum.ru

Journal Name

ARTICLE

1. Introduction

To achieve an economically feasible gas-to-liquid technology, it is necessary to meet several strict requirements, particularly a robust, highly productive Fischer-Tropsch (FT) catalyst, which would preferably be capable of producing low-wax syncrude in one step[1,2]. Because the FT process is highly exothermal, the product distribution depends essentially on operating temperature. In addition to that property, the actual temperature distribution in the catalytic bed affects the catalyst deactivation dynamics and its operating lifetime and finally determines the material balance of the integrated gas-to-liquid flowsheet. Thermal stability of a highly productive process is governed by a number of well-known factors, while the importance of thermal conductivity of catalyst pellets and the catalytic bed is critical[3,4].

The development of standard extruded pellets with high thermal conductivity[5] due to introduction of metallic aluminium and Raney cobalt and the implementation of a percolation system (by heat runoff) enabled us to create significantly more active catalysts compared with the existing ones. However, the high reactivity of aluminium metal may result in its degradation during the exploitation. If this degradation happens, the catalytic system would transform into conventional cobalt alumina catalysts with lower productivity.

This finding indicates that another, non-metallic thermally conductive component is highly desirable for future highly productive Fischer-Tropsch catalysts. Notably high thermal conductivity and good chemical stability of silicon carbide (SiC) make it an excellent candidate. It is important to notice also that the synthesis of β-SiC with high surface area has been reported[6,7,] while these studies[8,9] reported the synthesis of SiC extrudates or foams with open porosity[9] and specific surface area of several scores of metres.

Authors[9,10,11,12] used β-SiC (Sicat product) at 30 to 40 m^2/g as a support for the Fischer-Tropsch synthesis catalyst, while these studies[13,14,15,16] found that such catalysts manifest extraordinarily high activity and supreme selectivity for liquid hydrocarbons due to high SiC thermal conductivity (~5,5 W/(m·K)[16]. It is well-known that the composition and properties of the impregnated component and the support may change depending on preparation technique and conditions of pretreatment and activation. The formation of different catalyst phases and surface structures is possible depending on pretreatment support, catalyst synthesis conditions and precursor type [16].

This study undertook a thorough comparative physico-chemical characterization of β-SiC-supported Fischer–Tropsch synthesis catalysts, which exhibit different performance in catalysis, despite highly similar manufacturer specifications for supports, i.e., similar values for surface area and pore volume of supports.

2. Experimental

2.1 Sample preparation

Granulated silicon carbide was used as a support (Sicat LLC product specifications are shown in Table 1). The pore volume was measured by mercury porosimetry and pore size distribution by nitrogen physisorption.

In certain cases (Table 1, line 5) a pristine support was modified by the γ-Al_2O_3 layer coating technique. A pre-determined amount of $Al(NO_3)_3$*$9H_2O$ was introduced into the support by impregnation at 50°C; then, the impregnated sample was titrated with aqueous ammonia solution until pH=8 was achieved. The sample matured in the solution for one day; then, it was taken into the open air and calcined at the temperature that yielded the formation of γ-Al_2O_3 layer with surface area of approximately 200 m^2/g Al_2O_3.

The catalytic systems (18-20 % wt. Co^0) were prepared by one- or two-step incipient wetness impregnation of calcined (or pristine) supports with water (or ethanol) solution of cobalt nitrate with intermediate drying; one or two calcinations in air flow or without it. The cobalt concentration was calculated from precursor weight change; the chemical composition of hydrated cobalt nitrate or its oxides after appropriate temperature treatment was used.

The catalyst samples are identified by the following identifier:

αCo/(SiCε)-γ-xy-zT(τ)

where

αCo — Coº loading (wt.%) in theoretical catalyst composition (a sum of cobalt metal and dry support);

SiCε – pristine or modified SICAT support (see Table 2);

γ – temperature of support thermal treatment or “0” if no treatment was used;

x – number of impregnations;

y –solvent used (W for water, E for ethanol);

z – calcination type after second or only one impregnation (A for air flow conditions, O — without air flow, O** — helium flow).

T – calcination temperature, ºC;

τ – calcination period, hour.

Table 1. Support sample specifications as provided by the manufacturer

Support	Identification mark				
	SB0640F	SB0704B	DA0529C	DA0531L'	SB0640F modif.
	Short designation				
	SiC1	SiC2	SiC3	SiC4	SiC1 modif
Composition	β-SiC	β-SiC	β-SiC	$18Al_2O_3$-SiC	$0,17Al_2O_3$-SiC
Pellet diameter, mm	2	2	3	3	2
Surface area, m^2/g	25-35	25-35	25-35	25-35	-
Dominant pore size, A°		100	100+ 10000	-	-
Pore volume, ml		0,55	0,6	-	-

For example, sample 19Co/SiC2-0-2E-A550(1) was prepared by two-step impregnation of uncalcined pristine SBO704B support in ethanol solution of cobalt nitrate. The intermediate air calcination at 550 ºC and 1 hour conditions. Sample contains 19 wt.% of Coº in the assumption that catalyst weight is a sum of cobalt metal and waterless SiC2 support.

2.2 Sample characterization

Thermal conductivity of pristine supports and synthesized catalyst samples was measured from heat capacity at constant pressure data (DSC8000(Perkin Elmer)) and from temperature conductivity (NETZSCH LFA 457/2/G MicroFlash analyzer). It should be noted that cells with small-scale apertures for inlet and outlet laser emission were developed and used.

The effective thermal conductivity of porous silicon carbide extrudates (surface area ca. 30 m^2/g) should be 3,5-4,5 $W/(m\cdot K)$[11]. Thermal conductivity measured at temperatures ranging from 20 to 300ºC did not decrease by more than 20 %, while heat capacity increased by 20–25 %.

Thermal conductivity was calculated according to the formula:

$$\lambda = \acute{\alpha}\cdot C_p\cdot \rho,$$

where ρ — apparent density calculated from geometric parameters of sample, kg/m^3;

ά — temperature conductivity, m^2/s;

C_p — heat capacity, $J/(kg\cdot K)$.

The temperature conductivity of every material under investigation was measured for three representative samples with three independent measurements for each sample at every temperature. The accuracy of the measurements was better than 0.1 %.

The decrease in temperature conductivity at 220 to 250ºC is compensated by the increase of heat capacity, while thermal conductivity remained unchanged within 1 % (see Table 2).
Structural parameters of the pore system were examined by nitrogen physisorption with Autosorb-1C and helium pycnometer Ultrapyc 1200e (Quantachrome Instruments).

All sorption-desorption isotherms and pycnometry data were obtained in the physically same sample after the same sample preparation (thermal vacuum degassing at 300ºC) to eliminate any possible influence of heterogeneity of granular systems.

Catalytic systems were investigated at temperatures ranging up to 1000ºC by thermal programmed reduction at Autosorb-1C (equipped with catharometer). The oxidized precursor was a subject for thermal programmed reduction (TPR regime), while the sample pretreated under catalyst activation (which was then cooled down) was investigated in TPR-AR (thermal programmed reduction after reduction) regime. One can observe trace oxide phases (composition is close to realized in activated catalyst) reduced under such conditions.

Thermal gravimetric analysis of supports in air and in inert gas was performed with NETZSCH STA-449 F1 equipped with the chromatographic identification of emitted gas composition. The results were used for estimation of the behaviour of pristine supports and changes in phase and surface composition; this estimation also allowed for the simulation of sample modification at calcination.

Scanning electron microscopy (SEM) was done at JEOL JSM-7600F with local elemental analysis by energy dispersion spectroscopy (EDS).

2.3 Catalytic investigations

Fischer–Tropsch catalyst testing was performed in a stop-and-go regime (daily run of 6-8 hrs) by the technique described elsewhere[17]. This technique implies the synthesis in a fixed-bed tubular reactor with a non-diluted bed filled with catalyst granules (bed volume 2.5 cc, catalyst granules were 3 mm long and 3 mm in diameter in accordance with Table 1). The ½" tube was equipped with a radial thermowell (1 mm diameter), which allowed us to measure temperature in the centre of the bed. The reactor was equipped with a jacket, where a flow of pressurized boiling water circulated, which provided a very efficient control of the reaction temperature. The synthesis gas with H_2:CO ratio 2:1 was fed into the reactor at 2 MPa pressure. The catalyst was pre-activated in 0.1 MPa hydrogen flow for 1 hour at 400°C and GHSV of 3,000 h^{-1}. The activated sample was slowly driven to optimal synthesis conditions by stepwise daily increases of temperature by 3-6°C. Starting synthesis temperature was 170°C.The reactor was driven down to room temperature at the end of a daily run; the next run started at the next temperature step. After achieving maximum productivity at the GHSV of 1,000 h^{-1}, the GHSV was increased to check the catalyst performance at shorter contact times. The technique established that the optimal conditions were determined by the highest possible C_{5+} yield at chosen GHSV. This work, however, compares the results at nearly identical temperatures and GHSV to understand the role of surface cobalt structures.

3. Results and Discussion

3.1. Thermal conductivity

One can see that the pristine SiC1 support modification with alumina even in a thin surface layer (SiC1 modif.) results in a significant decrease in thermal conductivity of the sample, while the increase in γ-Al_2O_3 concentration (SiC4) leads to an even more significant decrease.

It should be noted that SiC1 and SiC2 supports, which are almost identical according to the manufacturer's specifications (see Table 1), are characterized by different thermal conductivity.

The change in the pore system and the increase in macropore content (i.e., the change in amount both of inner contacts and of pore body carcass elements) also lead to the decrease in thermal conductivity of porous, granular and fibrous materials[18]. As will be shown later, the structural parameters of SiC1 and SiC2 are slightly different, which may cause differences in thermal conductivity.

Table 2. Thermal conductivity of supports at Fischer–Tropsch synthesis temperatures

Sample	SiC1	SiC2	SiC3	SiC4	SiC1 modif.
Thermal conductivity, W/(m·K)	225°C				
	2,20	2,48	1,53	1,26	1,83
	250°C				
	2,19	2,44	1,54	1,24	1,84
Average thermal conductivity at 225–250°C, W/(m·K)	2,20	2,46	1,54	1,25	1,84

3.2. Thermal analysis

All β-SiC (SiC1–SiC3) samples are characterized by the decrease in weight at temperatures below 370ºC both in inert and oxidizing atmosphere (Fig. 1). This decrease is caused by simultaneous removal of hydrate–hydroxyl covering and oxidation of the intrinsic carbon (presumably residue after the support manufacturing procedure as indicated from weak vague exo-effect in the corresponding area). This results in insignificant (0.18 % for SiC2) weight loss with stabilization at 320–430ºC. Carbon removal as CO_x is compensated by oxygen coupling with possible formation of carbonate-carboxylate structures and support surface oxidation. Above 400ºC, the surface oxidation of samples 2 and 3 becomes predominant, and it results in a weight increase due to SiC oxidation forming surface silicates and hydrosilicates[13, 19] SiO_2 is generated in the surface layer and partially blocks SiC, thus preventing further oxidation of the carbide phase. Therefore, the air calcination of the support affects the surface to different extents depending on the temperature due to the formation of phases similar to SiO_2. Consequently, the support is quite stable to oxidation at conditions of Fischer–Tropsch synthesis. This also means that the air calcination at temperatures above 400ºC can be used for support surface modification with the formation of SiO_2/SiO_xC_y structures[9].

At the same time, significant differences occur with high-temperature oxidative treatment.

Heating of the SiC3 sample (X-ray diffraction analysis is the same as for SiC2) results in a lesser weight increase at a significantly higher temperature (748ºC). We believe that this finding is because SiC3 has a pre-oxidized surface with no carbon residue, which may influence the catalytic performance of the systems formed at these two supports.

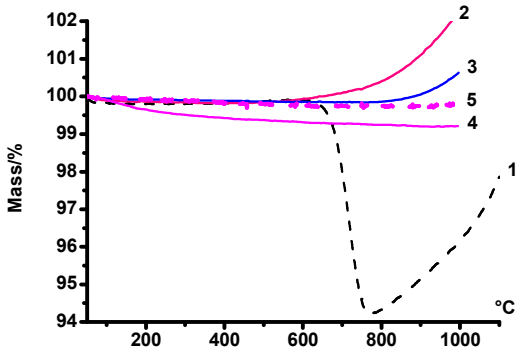

Fig. 1 Thermal gravimetric analysis of SiC1 (1), SiC2 (2), SiC3 (3), SiC4 (4) and 1 %Al2O3-SiC1 (5) supports in air (1-3) or helium (4, 5) flows

SiC1 support, which has the same phase composition, surface area and granule size as SiC2 support (the only difference is greater impurities content), is characterized by an intense exo-effect at 720ºC (Fig. 2) and a significant weight decrease (Fig. 1).

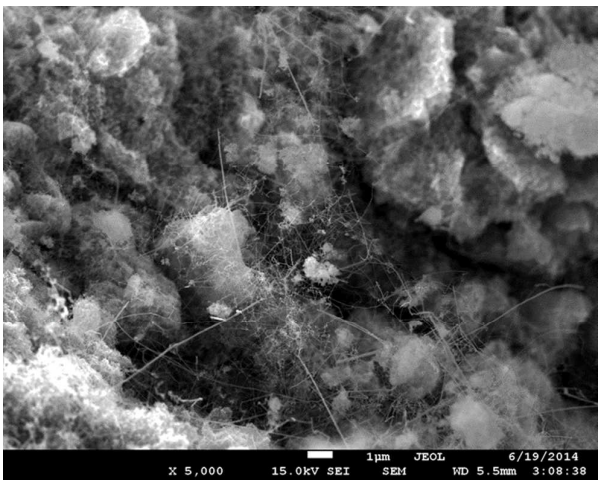

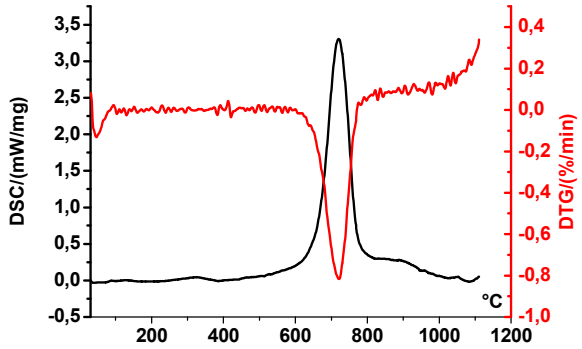

Fig. 2 DSC and DTG data for SiC1 support

It is obvious that a significant amount of carbon residue is oxidized, resulting in the reported exothermal effect. In contrast to SiC2, the carbon residue in SiC1 cannot be amorphous due to the position of the exothermal effect. The observation by scanning electron microscopy showed that the carbon residue of SiC1 has nanometric fibrous morphology, presumably carbon nanotubes.

a

b

Fig.3. SEM of carbon nanotube-populated surface of SiC1 support: (a) – general view of the nanotube network; (b) magnified view of nanotubes.

Fig.3 shows SEM of representative surface areas of SiC1 support. A network of surface-grown carbon nanotubes. The nanotube diameter varies 10 to 30 nm. EDS witnesses that the nanotubes are indeed carbon, i.e. the nanotube-populated areas contain substantial extra carbon in the quantities much higher than that in clean SiC surfaces.

Thus, the thermal analysis data show that very similar (see Table 1) silicon carbide supports are characterized by significantly different surface composition, thus pre-determining the formation of notably different catalytic systems on this basis.

The modified SiC4 and SiC1 supports showed quite different thermal analysis behaviour, namely, the only significant effect was the removal of loosely bound water at the temperatures below 200°C in a dynamic inert atmosphere and then dehydroxylation at approximately 1000°C. We believe that this because these supports were both modified by γ-Al_2O_3.

The heat treatment conditions of SiC1 modif. sample containing 0.17 % of γ-Al_2O_3 (not shown in Fig. 1) with a sample containing 1 % of γ-Al_2O_3 showed that the modification of the SiC1 support leads to formation of a thin surface layer of γ-Al_2O_3, silica, hydrosilicates and aluminosilicates, which form a protective surface layer on β-SiC.

This layer should contribute to better dispergation of catalytically active components on the catalyst surface. However, that same alumina layer leads to a decrease in thermal conductivity (see Table 2) due to essentially lower thermal conductivity of alumina compared to silicon carbide.

3.3. Pore structure

3.3.1. Supports

It is well known[20, 21, 22] that support structure and pore size distribution significantly affect diffusion and mass transfer properties and may determine both catalytic activity and Fischer–Tropsch synthesis selectivity.

The pore structure of supports (see Table 1 for the data specified by the manufacturer) was investigated to provide a more correct interpretation of the catalytic system testing data and an understanding of formation dynamics of precursors and catalysts.

Table 3. Structural characteristics of the support pore system

Characteristic		Support					
		SiC1	SiC2	SiC3	SiC4	SiC1 modif.	SiC1 *
S_{BET}, m^2/g		27,27	26,95	25,57	35,90	29,90	29,40
ρ, g/cm^3	Apparent	1,21	1,19	1,03	1,08	–	1,09
	True	3,15	3,47	3,24	3,39	–	3,77
Porosity, %	Open	61,7	68,4	61,2	68,2	–	71,2
Pore volume, cm^3/g	Total	0,51	0,62	0,66	0,63	–	0,66
	∑**	0,36	0,25	0,25	0,27	0,34	0,31
	BJH***	0,36	0,25	0,26	0,27	0,34	0,32
	Macropores	0,15	0,37	0,41	0,37	–	0,34
Macropore content, %		29,9	60,1	61,8	58,0	–	52,7

Remarks: *this SiC1 sample was air calcined at 600°C for 5 hours to determine weight loss after water contact (6 wt.%) with the purpose of comparing it with SiC1 modif. sample and to adjust the experimental weight of SiC1 modif. by this value.** Total pore volume for pores with diameter less than 230 nm at P/Po = 0.99. *** BJH method cumulative desorption pore volume.

Nitrogen sorption isotherms for SiC1, SiC2 and SiC3 supports correspond to the type of H1[23] isotherm according to IUPAC classification; this isotherm type is typical for meso- and

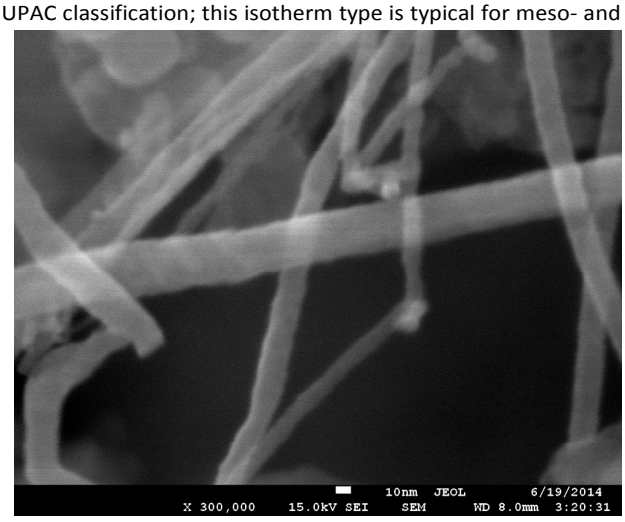

macroporous globular adsorbents. It is important to notice that neither of the examined supports possess any significant microporosity. Despite similar surface area values (Table 3), these supports have significant differences in macropores. While the total pore volume (in the nitrogen physisorption range) of SiC1 is greater than that of SiC2, the macropore volume is higher in the case of SiC2 (see Table 3). SiC1 sample adsorption is characterized by a maximum macropore area above 500 Å and a shoulder at 50 to 200 Å, while the SiC2 sample is characterized by a substantial increase in mesopore content; and, finally, in the case of SiC3 samples, the 80 to 120 Å pores become predominant. Modification of silicon carbide with large amounts of alumina leads to partial pore collapse, which results in the appearance of secondary porosity at 70 to 200 Å. Introduction of smaller amount of Al_2O_3 (Fig.4, lines 1, 5) results in weaker pristine support macropore depletion and secondary porosity formation.

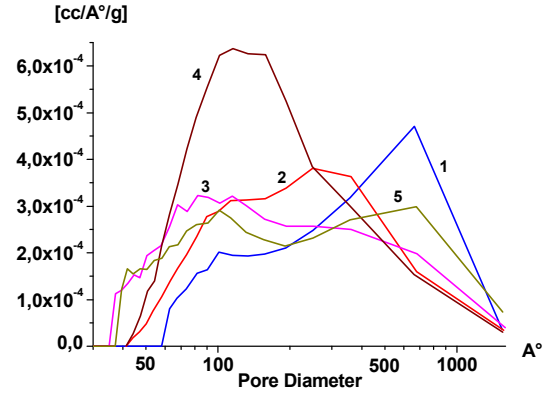

Fig.4. Pore size distribution for SiC1 (1), SiC2 (2), SiC3 (3), SiC4 (4) and SiC1 modif.(5) calculated from the BJH desorption isotherm line

It should be noted that the major modification of surface area and the porous system is achieved under conditions of thermal destruction of the sample (see SiC1 and SiC1*, Table 3), while the actual weight loss during air calcination and carbon decontamination is determined reliably by thermal analysis. As a result, investigated supports have significantly different properties despite very similar manufacturer specifications.

3.3.2. Catalysts

Catalysts prepared on pristine investigated supports are presented in Table 4. The pore structure modification process that takes place during active component deposition and catalyst precursor calcination is discussed below using an SiC1 support and Kat 1a catalyst as an example.

The decrease in integral pore volume due to the loading of the support structure with the active component and thermolysis products is observed in the presence of catalyst (Fig.5a). It is accompanied by appearance of secondary micro- and mesoporosity surface area (Fig.5b) due to cobalt component deposition. Surface pore size distribution is also affected (Fig.6).

Table 4. Catalysts and supports

№	Pristine support	Support designation	Catalyst designation	Catalyst identifier
1	SB0640F [β-SiC]	SiC1	**Kat 1a**	19Co/SiC1-0-2E-A750(1)
2			**Kat 1b**	20Co/SiC1-0-2W-A250(1)
3			**Kat 1c**	17,8Co/SiC1-0-2E-A550(1)
4		SiC1 modif.	**Kat 1d**	19Co/SiC1 modif.-0-1E2W-A250(1)
5	SB0704B [β-SiC]	SiC2	**Kat 2**	18Co/SiC2-450-1E-O550(1)

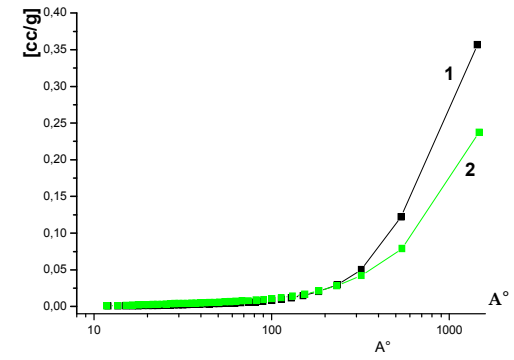

(a)

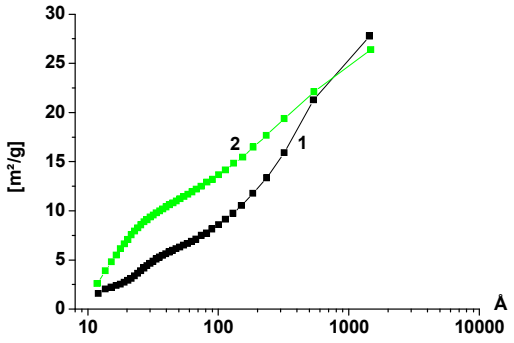

(b)

Fig.5. Integral pore size distribution of specific pore volume (a) and surface area (b) for SiC1 (1) and for Kat 1a (2)

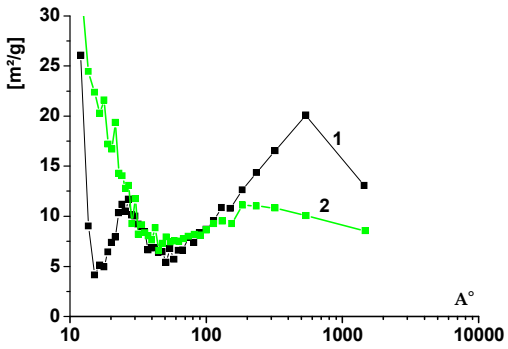

Fig.6. Pore size distribution of specific pore surface for SiC1 (1) and Kat 1a (2).

3.4. Temperature programmed reduction of precursors and Fischer–Tropsch catalytic systems

The understanding of catalyst surface phases and structures is desirable to achieve higher catalyst productivity and selectivity. It is well known, for example, that Co/Al_2O_3 catalytic systems can be characterized by the presence of a number of intermediate states, which may include either bulk Co° or dispersed Co[24]. As suggested[25] and supported[21], a partly reduced cobalt plays a special role. Particularly, it was shown[26] that only one cobalt-oxide phase, which is characterized by specific maximum at TPR, is responsible for liquid hydrocarbon formation during FT synthesis. These phases represent the structures immobilized on the support surface. These structures comprise metal Co° atoms localized at CoO_x particles. The interaction of the reduced metal with oxide (in the framework of such site) results in electron density shift, causing cobalt effective positive charge acquisition, so the $Co^{\delta+}$containing phases[25] can act as selective catalytic sites for Fischer-Tropsch synthesis.

Catalytic systems and theirs precursors were studied by the TPR method to investigate the formation of cobalt-containing phases.

3.4.1. Systems based on SiC1 support

TPR data of catalytic systems based on the SiC1 support presented in Fig.7 indicate significant differences depending on the catalyst formation route. High temperature calcination of SiC1-based catalysts results in a drastic decrease in surface cobalt ion content (seen from the high temperature peak) and immobilized cobalt oxide structures (seen from the observed transition between a broad maximum and a shoulder at 500 to 600°C). This effect can occur due to high temperature oxidation of support into silica and the formation of non-reducible cobalt silicate and hydrosilicate surface phases.

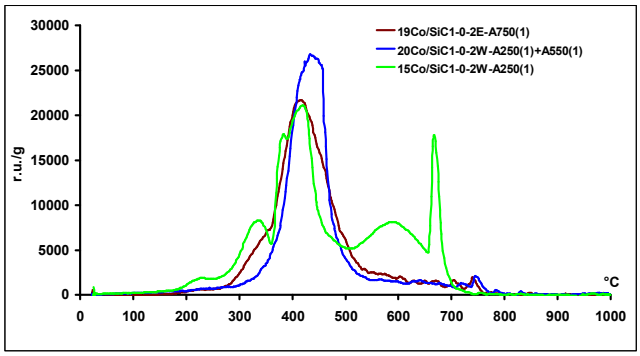

Fig.7. TPR data for catalytic systems based on SiC1 support prepared by aqueous (or ethanol) solution impregnation

3.4.2. Systems based on SiC2 support

Fig.8 represents TPR data from SiC2-supported catalysts. This system was prepared by single incipient wetness impregnation of a SiC2 support previously calcined at 450°C with cobalt nitrate hexahydrate; it was then heat treated at different temperatures (450, 650 and 1000°C) under air flow. The Hedwal principle[27] was used to interpret the observed effects. Hedwal states that reaction kinetics change near the phase transition point. Applying that principle to our case, the position of an observed maximum corresponds to the change in reduction reaction or reductive decomposition kinetics (the reductive decomposion occurs with release of H_2O and NO_x).

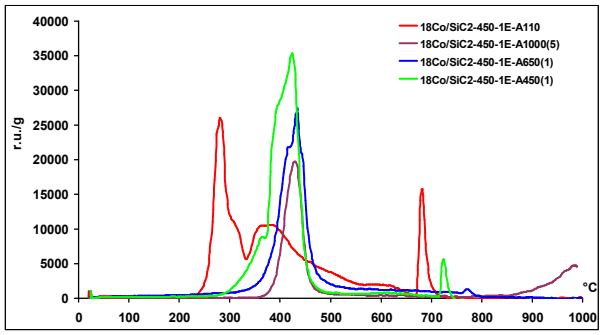

Fig.8. TPR data for the pristine catalyst precursors and those calcined at 450, 650 and 1000°

Comparison of obtained data with literature allows to identify the resulting phases, structures or surface states of cobalt containing component.

The peak with a maximum at 260°C corresponds to reductive decomposition of $Co(NO_3)_2$ in the presence of uncalcined 18Co/SiC2-450-1E_110. The peak shift from 180°C (typical temperature for dry bulk cobalt nitrate)[28] to 260°C is a result of nitrate binding to surface hydroxyls (perhaps of hydroxysilicate origin) and decomposition with a hydrated Co_2O_3 nonstoichiometric composition and the formation of cobalt oxide hydroxycomplexes (shoulder at 300°C)[29]. Hydrogen absorption at 360°C and 380°C as well as a shoulder at 450 to 550°C are caused by gradual reduction[30] of massive

differently sized agglomerates of the Co_3O_4 phase, which is a solid solution of CoO in Co_3O_4. The broad maximum at 550 to 650°C corresponds to the reduction of multilayer cobalt oxide phases immobilized at the support surface. The nature of the intensive narrow maximum at 650 to 800°C will be discussed later.

Different behaviour is observed for calcined samples. All low temperature maximums corresponding to crystallohydrate decomposition disappear. The Co_3O_4 reduction maximum shifts to the higher temperature area (420°C). TPR of the calcined samples indicate a calcination-induced transition of the cobalt nitrate phase into surface oxide agglomerates. The amount of Co_3O_4 phase grows significantly, but the increase in calcination temperature leads to a decline in Co_3O_4. Reduction peaks at 360 and 380°C for 18Co/SiC2-450-1E-A450 indicate the presence of remaining low temperature phases, which are not observed for the samples calcined at higher temperatures. The increase in temperature in 18Co/SiC2-450-1E-A450 and 18Co/SiC2-450-1E-A650 results in cobalt redistribution on the support surface with the formation of immobilized phases, which are selective in long-chain C_{5+} hydrocarbon production[26]. However, excessively high calcination temperatures lead to the formation of hardly reducible surface and subsurface structures. As a result, some cobalt sites are not involved in catalysis (for example 18Co/SiC2-450-1E-A1000).

Thus, the quantity and quality of resulting cobalt phases can be controlled by variations in the heat treatment temperature. Appropriate calcination temperature ensures efficient cobalt distribution and support surface binding.

Sharp hydrogen consumption maximums of different intensities are observed from TPR data at 650–750°C in the presence of investigated precursors. The appearance of such maximums is not typical for cobalt alumina Fischer–Tropsch synthesis catalysts. The observation of such effects was reported in the presence of heavily loaded cobalt catalysts (up to 60 % wt. of Co^0) based on zeolites and silica[31].

Special experiments were performed to establish that these peaks were not the result of desorption of intrinsic surface groups. It was shown that such groups appear *only after deposition of the cobalt-containing component*, indicating its special interaction with the support surface during the impregnation. Thus, it shows the reduction of the surface cobalt-containing phase is related to that formed on silicon oxide. Their presence was confirmed by DTA-TG data that shows thin surface layer oxidation (during active component deposition and catalyst calcination) of silicon carbide to silica. Decreases in intensity and peak shift to higher reduction temperatures (with the increase in precursor calcination temperature) suggest the intensification of the cobalt interaction with such fixation sites. It also suggests that some cobalt sites migrate to other more strong surface fixation sites. Otherwise, the calcination temperature increase would result in increases of this phase intensity due to decreases in cobalt content (Fig.7) in agglomerated phases with a reduction maximum at 460°C. Infrared spectroscopy and X-ray diffraction methods show[32] that this surface phase on cobalt-zeolyst systems is similar to cobalt silicates in which cobalt is bonded with one- or two-bridge oxygen. These data are in agreement with both the presence of a surface SiO_xC_y layer declared by the manufacturer[9] and with surface silicon carbide oxidation discovered in our experiments. The peak intensity decreases with the increase in calcination temperature (Fig.8), and 18Co/SiC2-450-1E-A1000 was characterized by zero intensity. Significant hydrogen consumption occurs at 950-1000°C, suggesting that cobalt migrates to form structures which are more strongly fixed on the support surface. Some cobalt particles will fix on other sites due to diffusion forming surface and subsurface phases, which are not reduced at investigated temperatures and cannot be observed by the TPR method.

It was shown that not only calcination temperature but also calcination atmosphere influences the quality and quantity of cobalt surface structures (Fig. 9). TPR data for catalysts after calcination in air or in an NO_x atmosphere differ significantly.

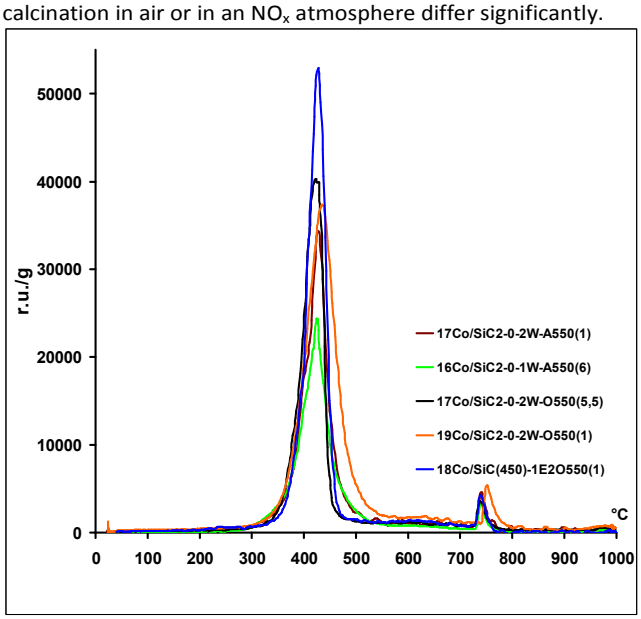

Fig. 9. TPR data for catalysts after calcination in air or in NO_x atmosphere

The samples investigated in this experiment were calcined at 550°C, which causes decomposition of hydroxyl-containing cobalt oxide phases and eliminates low temperature reduction effects on the TPR line. Only massive Co_3O_4 phase is detected at the catalyst surface. All samples were characterized by the same reduction temperature of this phase, but peak shape and intensity have significant differences.

17Co/SiC2-0-2W-O550 as compared to 17Co/SiC2-0-2W-A550 was characterized by higher maximum intensity at 440°C (in accordance with higher content of the phase reducible at this temperature). Nearly the same reduction maximum intensity of 16Co/SiC2-0-1W-A550 and 17Co/SiC2-0-2W-A550 indicates a similar content of agglomerated Co_3O_4 phase. Therefore, the catalyst precursor thermolysis after aqueous solution impregnation (for 17Co/SiC2-0-2W-A550) does not result in a significant increase of cobalt surface sites. The

reduction peak of massive oxide after heat treatment in NO_x becomes more narrow when the heat treatment time is longer (Fig. 9). This fact indicates fewer fixation sites and greater dispersion homogeneity of cobalt oxide. 18Co/SiC2-450-1E-O550 has the highest intensity of this maximum. This sample was prepared by single impregnation with ethanol cobalt nitrate solution on a pre-calcined support. The peak is more narrow than that observed in the presence of 19Co/SiC2-0-2W-O550. One can conclude that support pre-calcination or calcination during sample preparation at 450 to 550°C causes this phenomenon.

The use of ethanol as a solvent promotes effective and uniform fixation of cobalt-containing components on the support surface with the formation of additional fixation sites and cobalt dispergation. The use of ethanol cobalt nitrate solution and its careful evaporation at low temperatures avoids the capillary removal of salt, agglomeration effects for cobalt nitrate decreases compared to water evaporation. This results in greater intensity of the high temperature maximum (compared to two-step aqueous solution impregnation) and its relative shift to lower temperatures. A similar conclusion was made in a study[33] in which the ethanol solution impregnation of SiC supports led to the formation of Co-Ru particles smaller than 8 nm. However, the amount of excess regarding the support interaction and agglomerated Co_3O_4 phase was significantly higher in cases of ethanol impregnation.

It is clear from thermal analysis data of SiC2 supports that the surface SiO_2 phase is formed during the oxidation process. 16Co/SiC2-0-1W-A550 and 17Co/SiC2-0-2W-O550 are characterized by different TPR intensities, which cannot be explained by differences in the quantity of cobalt content. TPR maximums are very close for 16Co/SiC2-0-1W-A550 and 17Co/SiC2-0-2W-O550 samples. Therefore, calcination in NO_x atmosphere leads only to a quantitative increase in reduced agglomerated cobalt oxide phases. Support surface modification with nitrogen oxides slightly increases cobalt's interaction with surface support active sites and results in the formation of smaller amounts of fixation sites in comparison with support (catalyst) during air calcination under the same conditions. Surface silicate phase is reduced in 18Co/SiC2-450-1E-O550 samples at the temperature typical for air calcined precursors. In other words, calcination in a nitrogen oxide atmosphere causes no change in fixation sites formed after air calnication. The content of surface hydroxyl-containing sites decreases, forming greater amounts of Co_3O_4 agglomerates.

The formation of surface cobalt-containing phases and structures on pristine SiC2 support during the increase in cobalt concentration is presented in Fig.10. In the presence of impregnated 10Co/SiC2-0-1W agglomerated and surface cobalt-containing phases (which are typical for catalysts based on this support) are formed, even after primary drying (see discussion in Fig.8). Intensive maximum at 270°C is a sum of cobalt nitrate and cobalt oxide hydroxycomplex reduction effects and demonstrates the effective salt component fixation on the support surface. The shoulder at 300°C indicates partly hydrated Co_2O_3 reduction with the simultaneous formation of massive Co_3O_4 crystallites. The latter became partly reduced to CoO at 320°C. Solid solution CoO-Co_3O_4 formed at the support surface has a broad reduction maximum at 350 to 500°C. The shoulder observed at 550 to 650°C indicates Co° formation from the surface CoO_x multilayers. High temperature peaks at 670°C, which are comparable to the peak of crystallohydrate reduction, is attributed to the reduction of high amounts of isolated cobalt ions weakly fixed on silica-oxide surface sites.

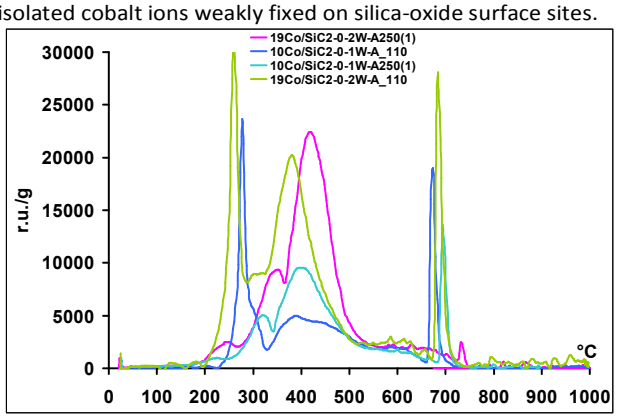

Fig. 10. TPR data for catalyst precursors based on uncalcined support (water impregnation)

The sample air-calcined at 250°C is characterized by the presence of residual hydrated Co_2O_3 nonstoichiometric phase (230°C) and cobalt nitrate and the results of its decomposition into massive agglomerates, which are effectively reduced with CoO into Co_3O_4 (350-500°). Reduction of the maximum intensity of excess massive oxide phase increases with calcination and becomes more narrow, which indicates a smaller range of agglomerated phase particle size distribution. It should be noted that in spite of growth in the Co_3O_4 agglomerates content, CoO_x surface phase content remains the same before and after calcination. Surface cobalt phase remains in the oxide form and is strongly fixed at the surface, where so no migration occurs. Support pre-treatment determines surface group content. Formation of this phase takes place during cobalt nitrate impregnation and primary drying, as confirmed by increases in this phase content after second impregnation. The decrease in this maximum intensity as a result of precursor calcination is caused by cobalt redistribution to other phases (including subsurface phases) and fixation with the support.

The TPR line for 19Co/SiC2-0-2W-A110 is similar to that of 10Co/SiC2-0-1W-A110 (except cobalt nitrate reduction decomposition at low temperature range). The observed intensity increase is caused by superposition of previously formed cobalt-containing phases with newly formed ones. Second impregnation results in a significant increase in the intensity of high-temperature reduction peaks of cobalt silicate structures, and some shift to lower temperatures was observed. Obviously this phase is also the surface phase, and it is formed during cobalt nitrate's interaction with surface support groups. Even low temperature calcination of 19Co/SiC2-0-2W-A250(1) leads to the growth of agglomerated cobalt oxide content due to the decrease of isolated cobalt

ions fixed on silanole groups; however, the level of multilayer structures reduced at 500-650°C remains almost the same. Aqueous solution impregnation and air calcination at low temperature (250°C) of intermediate sample do not cause formation of fixation sites.

3.4.3. Systems based on SiC4 support

It should be noted that support modification does not affect the reductive decomposition of excess salt (Fig. 11), but γ-Al_2O_3 introduction blocks some surface sites of the silicon carbide support that could transform into silicon oxide structures. Therefore, the cobalt ions are fixed at small amounts of the remaining strong sites (or formed alumina silicate centres) that lead to the shift of the high temperature peak (Fig. 11). The introduction of γ-Al_2O_3 in the support composition dramatically decreases thermal conductivity (Table 2) and significantly changes the conditions of surface cobalt phase formation (Fig. 12). The system is similar in alumina-based catalysts, and the impact of surface protospinel cobalt aluminate structures increases. Silica or formed alumosilicate bunches located on remaining γ-Al_2O_3-free silicon carbide surface led to formation of a high temperature peak.

.

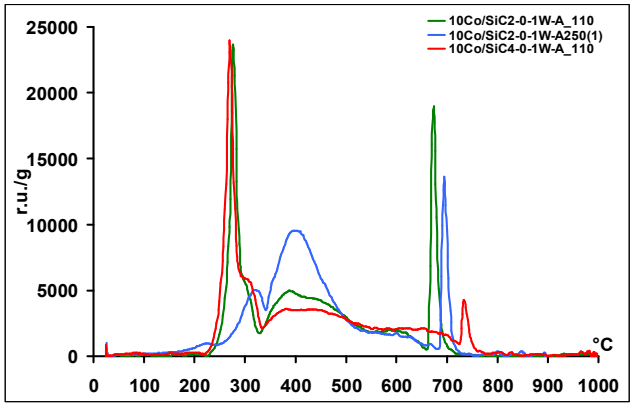

Fig. 11. TPR data for one-step impregnated systems based on SiC2 and modified with γ-Al2O3 SiC4 supports

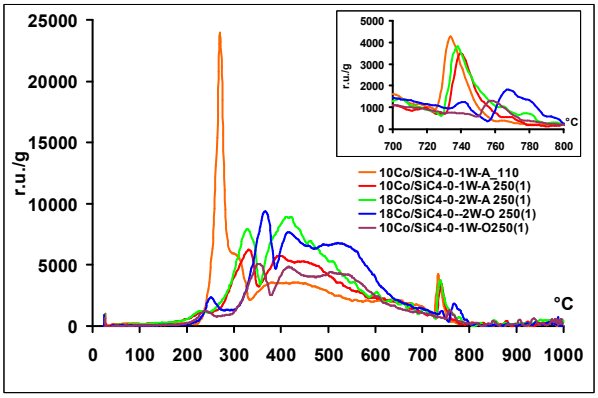

Fig. 12. TPR data of catalytic systems (aqueous solution impregnation) based on modified by γ-Al_2O_3 SiC4 support

It should be noted that the above-mentioned influence of air and NO_x calcination atmosphere is obvious in this case. The impact of isolated surface cobalt ions decreases and the content of immobilized multilayer structures reducible at up to 600°C increases. The content of immobilized and stronger fixed structures (600–700°C) changes insignificantly

3.4.4. The influence of differences between SiC1 and SiC2 supports on formation of catalytic systems

As mentioned above, preparation conditions have a significant influence on cobalt-containing precursor interaction with the support surface and result in the formation of different surface phases. The differences between SiC1 and SiC2 supports are very similar if judged from the manufacturer's specifications.

These differences result in essential differences in TPR data (Fig. 13), even for samples prepared in the same conditions and by the same technique. As noted above (Table 3), these supports differ in total pore volume (which is 20 % less for SiC1), in macropore volume (which is 2 times smaller for SiC1) and in mesopore volume (which is 1.5 times higher for SiC1).

Supports differ significantly in their chemical properties and in the ability to interact with cobalt-containing components, despite their similar total BET surface area. A shift in the TPR maximum at 150–450°C (with no change in shape) was observed for agglomerated structures, which indicates minor differences in the amount or size of formed crystallites. However, significant differences in peak shapes are observed at 500–650°C for surface structures. The reduction peak of the immobilized support CoO_x phase in the presence of 17Co/SiC2-0-2W-A250 sample has a plateau shape, while in the presence of 15Co/SiC1-0-2W-A250, the same phase appears as a broad peak with high intensity. It should be noted that these differences are observed for catalysts with comparable content of impregnated active components. As mentioned above, this phase is formed by cobalt nitrate's interaction with support surfaces during the impregnation process. The possible increase in this structure content due to the 20 % larger surface area of SiC1 support mesoporosity seems unlikely because the intensity of the TPR maximum is significantly higher (Fig. 13). The obtained results correlate with the aforementioned shift in the reduction maximum of massive structures in the presence of SiC1 compared to SiC2 and indicates the greater amount of these structures (despite the lower concentration of impregnated components) over dispersion differences. The

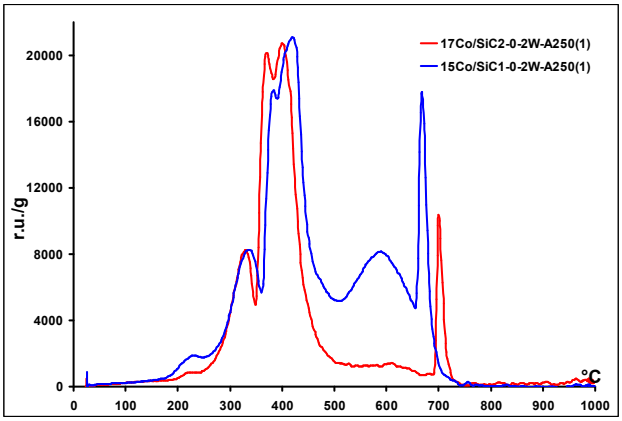

Fig. 13. TPR data of catalysts based on SiC1 and SiC2 supports calcined at 250°C

total excess of reduced cobalt observed in the presence of 15Co/SiC1-0-2W-A250 at 2 % lower catalyst metal loading indicates a weaker interaction with the support in the presence of SiC1. Cobalt nitrate is converted into the oxidizing melt in crystallohydrate water during the catalyst formation. Lower amounts of reducible and higher amounts of irreducible cobalt phases are formed in the presence of SiC2 support (Fig. 13). This suggests that the SiC1 surface has a higher oxidation resistance compared to SiC2, and this suggestion correlates with the existence of nanocarbon structures in SiC1's composition.

3.4.5. The influence of structure and surface support properties on catalyst genesis

The investigation of SiC supports and catalyst genesis on their basis enabled the preparation of samples (Table 4) further tested in Fischer–Tropsch synthesis. The choice of particular SiC supports and their pre-treatment conditions were performed in a way to have a set of catalyst samples with the maximum presence of the surface structures that are active and selective in C_{5+} hydrocarbon synthesis structures.

The formation of the catalyst occurs not only during active component impregnation and appropriate treatment but also during catalyst reduction and running.

Fig. 14 represents TPR data and Fig. 15 represents TPR-AR data obtained after sample pre-reduction in situ in device cells and further TPR of residual oxide phases and structures.

Heat treatment in a hydrogen atmosphere results in almost complete reduction of agglomerated cobalt oxide structures and partial reduction of surface immobilized phases.

We investigated the state of cobalt-containing components in detail with the example of Kat 1b.

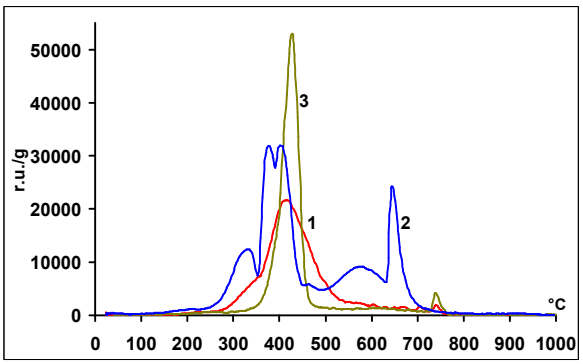

Fig. 14. TPR plots of systems tested in catalysis (1-Kat 1a, 2-Kat 1b, 3-Kat 2).

Catalyst Kat 1b was prepared by two-step aqueous solution impregnation of SiC1 with cobalt nitrate with intermediate heat treatment with air flow at 250°C. TPR data are characterized with residual structures of hydrated Co_2O_3 (peak at 300°C), massive cobalt oxide agglomerates of different sizes (maximums at 370 and 420°C), multilayer surface CoO_x (530–630°C) and immobilized cobalt ions (above 650°C). The reduction of Kat 1b leads to the formation of the structures atypical for cobalt oxide; they are characterized by hydrogen consumption maximums at 150°C. However, the multilayer CoO_x surface structures at 500 to 650°C are partially reduced, and the reduction maximum of surface cobalt silicate shifts to higher temperatures (as compared to pristine unreduced samples).

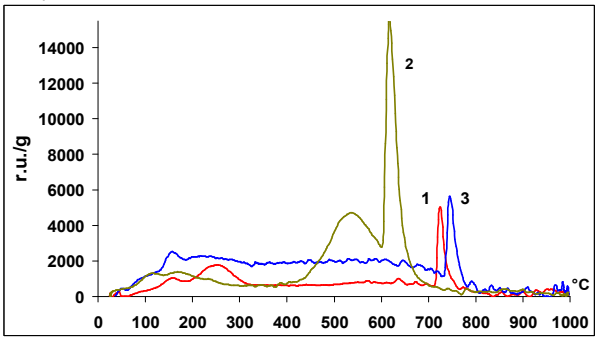

Fig. 15. TPR-AR plots of tested in FTP systems (1-Kat 1a, 2-Kat 1b, 3-Kat 2).

It should be noted that TPR intensity is comparable to TPR-AR intensity at high temperature ranges (Fig. 14, 14), which means that formed surface cobalt oxide phases remain in the catalytic system, although they undergo some transformations. Moreover, the reduction treatment of Kat 2 results in the increase of the amounts of such phases.

The reduction of massive Co_3O_4 agglomerates (300–500°C) and cobalt silicates (740°C) is observed in the presence of Kat 1a samples after high temperature treatment (750°C) in air flow (Fig. 14). TPR-AR data correspond to the same maximum at 150 and 250°C, similarly to the Kat 1b sample (Fig. 15). The high temperature peak shifts to 725°C; it is characterized by increased intensity as compared to reduction (Fig. 14). It seems likely that the prepared catalyst will contain relatively

high amounts of bulky massive cobalt agglomerates on the surface of unreduced cobalt silica oxide phase formed during the first impregnation. However, Kat 1 is characterized by a significantly lower amount of immobilized oxide phases reduced at 500–650°C (Fig. 14) than the Kat 1b sample. Kat 2's surface structure is characterized by hydrogen consumption maximums at 350 to 450 and 740°C. The major amount of cobalt is contained in the Co_3O_4 phase, which promotes the formation of large cobalt metal particles after reduction. The active sites of Kat 2 will primarily present with large cobalt agglomerates. Kat 1a and Kat 2 are characterized by lower amounts of unreducible oxide structures compared to Kat 1b, which is characterized by significant contents of multilayer cobalt oxide and cobalt silicate surface phases.

The cobalt-containing structures in catalyst composition indicated by the TPR method may be summarized as:

- cobalt oxide agglomerates of different dispersions;
- cobalt immobilized on the surface as CoO_x multilayer;
- surface silicates and hydrosilicates Co-SiO_x with degrees of different order.

Oxide structures of Co°/CoO_x, which are active and selective in Fischer–Tropsch synthesis of liquid hydrocarbons and are immobilized on cobalt catalyst structures, consist of reduced cobalt immobilized on oxide cobal- containing base, which is connected to the support surface. Electron density shift from metal to support occurs in this structure and the catalytic site can be represented as partially reduced cobalt with an effective $Co^{\delta+}$ charge.

Thus, Kat 1b and Kat 1a would show the best results ***if the structure characteristics and thermal conductivity of catalysts based on β-SiC were the same***. Kat 2 has a significant content of agglomerated cobalt phase, which promotes the formation of methane, CO_2 and gaseous hydrocarbons. It should be noted that reduced metal cannot be identified by the TPR-AR method, but the higher the cobalt dispersion and the amount of immobilized cobalt oxide at the support surface, the higher the number of such sites formed.

TPR-AR data represent maximums at temperatures up to 300°C, which are not typical for Co^{+2} or Co^{+3} reduction. It is likely that $Co^{\delta+}$ formation is accompanied by a negligible charge transfer and weak interaction with oxygen, reflected in TPR data as reduction maximums at temperatures extremely low for the reduction of known cobalt oxides. The reduction peak at 150°C, which does not appear in pristine precursors, is observed; it may be caused by different reasons, such as:

- $Co^{\delta+}$ formation on the surface of massive metal due to cobalt re-oxidation by water vapour during the reduction;
- metal re-oxidation by surface hydroxyl groups formed during the reduction due to the diffusive migration of cobalt crystallites on catalyst surface;
- dissociative adsorption of hydrogen on previously formed metal cobalt and atomic hydrogen spillover to surrounding cobalt-containing oxide components with further reduction at lower temperatures.

3.5. Testing of catalysts of different origin in Fischer–Tropsch synthesis

The β-SiC supports, which show similar surface area and X-ray diffraction patterns but differ in other properties, may manifest different catalytic performance. One expects stronger differences in catalytic performance for the samples, which are characterized by stronger differences in catalyst formation parameters.

Indeed, the results of experimental testing, which are shown in Table 5, demonstrate that differences in particular cobalt-oxide phases present in the sample, as well as differences in the dispergation of such phases, critically influence the catalytic performance, especially the achievable maximum yield of the product. Therefore, the approach applied in this work may be useful for the optimization of the catalyst manufacturing procedure for Fischer-Tropsch synthesis catalysts.

As mentioned in 3.4.5, Kat 1b and Kat 1a would show the best results if the structure characteristics and thermal conductivity of catalysts based on β-SiC were the same.

At the same time, Kat 2 has smaller amount of unreduced oxide structures after reduction compared to Kat 1b which is characterized by significant amount of multilayer cobalt oxide and cobalt silicate surface phases. It is necessary to note that laboratory-scale catalytic testing provides very low linear gas velocities, which makes the influence of thermal conductivity of the catalyst granules notably important for the performance of the catalyst, which is why the structure and thermal conductive differences of investigated systems slightly change the expected activity range of catalysts.

Kat 1a has the highest productivity in liquid hydrocarbons; all silicon carbide-based systems are characterized by smaller amounts of olefins compared with conventional Fischer–Tropsch synthesis catalysts.

Table 5. Catalytic performance

№	Sample	C_{5+}, g/kg·h	S_{C5+}, %	C_{5+} composition, wt. %.			α	Q (CO:H_2=1:2) h^{-1}
				Olefins	n-paraffins	iso-paraffins		
1	Kat 1a	327	45	8	78	14	0.73	5000
2	Kat 1b	233	40	6	81	13	0.77	4000
3	Kat 1c	121	55	5	88	7	0.82	3000
4	Kat 1d	190	44	11	77	12	0.78	4000
5	Kat 2	178	22	8	78	14	0.75	5000

Another important observation is that such high productivity was registered at the undiluted granular fixed bed, while the observed α ≈0,7-0,8 promised the direct synthesis of light liquid hydrocarbons, allowing us to skip the usual

hydrocracking step. The latter consideration may be important from a practical point of view.

4. Conclusions

It was determined that the catalysts based on SiC supports, which are characterized by highly similar surface area and pore volume, still perform differently in Fischer-Tropsch synthesis if the catalyst formation procedure leads to differences in the surface phase composition and active phase dispersion. The SiC supports may carry residual carbon in the form of either amorphous carbon phase or carbon nanotubes. The factor of the residual carbon determines different behaviour during oxidative treatment and differences in pore system and thermal conductivity.

It is possible to control the diversity and content of various cobalt-oxide phases, as well as the efficiency of cobalt distribution at the support surface. The quantity and quality of resulting cobalt phases can be controlled by the temperature variation in heat treatment. Appropriate calcination temperature ensures efficient cobalt distribution and support surface binding. The use of ethanol in the impregnation process provides more uniform cobalt distribution and better dispersion.

It was demonstrated that the contribution of isolated surface-bound cobalt ions decreases if calcination is performed in the presence of nitrogen oxides; the amount of immobilized multilayer cobalt oxides, which are characterized by complete reduction in hydrogen below 600°C, increases compared with calcining in air.

Further optimization of the catalysts can be performed on the basis of reported findings because the dynamics of surface cobalt phase formation and conversions enable the elaboration of optimized SiC-supported catalysts.

Acknowledgments

We gratefully acknowledge Sicat LLC for providing the sample, Bagramov R.Kh. for measuring the heat capacity of samples, Khaskov M.A. for providing DTA-TG data, Ivanov L.A. for providing SEM data, Asalieva E.Yu. and Sineva L.V. for carrying out the catalytic experiment, and Patrick Nguyen for his support and positive attitude.

Notes and references

[1] I.S. Ermolaev, V.S. Ermolaev a, V.Z. Mordkovich, Theoretical Foundations of Chemical Engineering, 2013, **47**, 153–158.

[2] I.S. Ermolaev, V.S. Ermolaev, V.Z. Mordkovich, Industrial & Engineering Chemistry Research, 2014, **53,** 2758–2763

[3] R. Philippe, M. Lacroix, L. Dreibine, Cuong Pham-Huu, D.Edouard ,S. Savin, F. Luck d, D. Schweich, Catalysis Today 2009, **147**,305–312

[4] Y.Liu,O.Ersen,C.Meng,F.Luck, Cuong Pham-Huu,ChemSusChem,2014,**7**,1218-1239

[5] V.Z. Mordkovich, Ya.V. Mikhailova, S.A. Svidersky, L.V. Sineva, I.G. Solomonik, WO/2008/079051;

V.Z. Mordkovich, L.V. Sineva, I.G. Solomonik, V.S. Ermolaev, E.B. Mitberg, Russian pat. #2405625 RU

[6]ZHAN Ying-Ying, CAI Guo-Hui, ZHENG Yong, SHEN Xiao-Nv, ZHENG Ying, WEI Ke-Mei, Acta Phys.Chim. Sin. 2008, **24** 171-175

[7] LIU Shui-gang, GAO Wie, Industrial Catalysis, 2005, **13**, 60-64

[8] Marc J. Ledoux and Cuong Pham-Huu, Cattech. 2001,**5** 226-246

[9] Patrick Nguyen, Charlotte Pham, Applied Catalysis A: General. 2011, **391**, 443-454

[10] Pham-Huu Cuong, M. J. Ledoux, S. Savin Poncet, *TOTAL France* FR 2864532

[11] S. Savin Poncet, M. J. Ledoux, Pham-Huu Cuong, J. Bousquet, B. Madani. *TOTAL France WO 2005/073345*

[12] Pham-Huu Cuong, B. Madani, M. Lacroix, L. Dreibine, M. J. Ledoux ,S. Savin Poncet, J.Bousquet, D. Schweich , *TOTAL S.A. WO 2007/000506*

[13] A. R.de la Osa, A.de Lucas, Luz Sanchez-Silva, J. Diaz-Maroto, J. L.Valverde.,
P.Sanchez, Fuel. 2012, **95**, 587-598

[14] . R. de la Osa, A. de Lucas, A.Romero, J.L. Valverde, P. Sánchez ,Catalysis Today.2011, **176**, 298-302

[15] A. R.de la Osa, A.de Lucas, J. L.Valverde., G.Vargas, J.Diaz-Maroto,
P.Sanchez, SynFuel2012 Symposium, 29-30 June 2012, Munich, Germany,P.382

[16] B.de Tymowski,"Fisher Tropsch synthesis on conductive silicon carbide based support",Ph.D..2012

[17] L.V.Sineva, V.Z.Mordkovich, E.Yu.Khatkova, Mendeleev Communications. ,2013, **23,** 44-45

[18] Thermal Conductivity ,Terry M.Tritt (ed) in "Physics of Solid and Liquds",2004,p.290, Springer

[19] R.Moene,M.Makee,J.A.Moulijn,Appl.Catal.A,167,1998,231-330

[20] G.V. Pankina, P.A. Chernavskii, G.P. Muravjeva, V.V. Lunin, Vestnik Moskovskogo Universiteta, ser.2, Chemistry, 2003, **44** 372-375

[21] E.Iglesia, S.L.Soled, J.E,Baumgartner, S.C.Reyes, J.Catal. 1995, **153**, 108-122

[22] A. P.Savost'yanov, V. G. Bakun, Russian Journal of Applied Chemistry.,2006, **79** ,1839-1843

[23] Rolando M.A. Roque-Malherbe, ,Adsorption and diffusion in nanoporous materials, CRC Press Taylor & Francis Group,2007

[24] W.H. Lee, C.H.Bartolomew, J. Catal. 1989. **120**, 256

[25] A.Lapidus, A.Krylova, J.Rathousky, A.Zukal, M.Jancalkova, Appl.Catal.A:General,1992,**80, 1-11**

[26] I.G.Solomonik, L.V.Sineva, V.Z.Mordkovich, Abstract , Int.Conf. MRC-IX,2012.267

[27] Ch.Satterfield ,Heterogeneous Catalysis in Practice, McGraw-Hill chemical engineering series, 1980, 416 p

[28] P. Rabu, S. Angelov, P. Legoll, M. Belaiche, M. Drillon, Inorg. Chem., 1993, **32** ,2463-2468

[29] Y.Okamoto, T.Adachi, K.Nagata, M.Odawara, T.Imanaka , Applied Catalysis ,1991, **73**, 249-265;

Y.Okamoto, K.Nagata, T.Adachi, T.Imanaka, K.Inamura, T.Takyu, J. Phus.Chem., 1991, **95**, 310-319

[30] P. Arnoldy, J.A.Moulin,J.Catal., 1985, **93**, 38-54

[31] I.G. Solomonik, report for RFBR grant, № 99-03-32172

[32] Sung-Jeng Jong, Soofin Cheng, Applied Catalysis A: General., 1995, **126**, 51-66

[33]B.Tymowski.Y.Liu,C.Meny,C.Lefevre,D.Begin,P.Nguyen,Ch.Pham,D.Edouard,F.Luck,Cuong Pham-Huu,Appl.Catal A^General,2012,**419-420**,31-40